NANOSYSTEMS: PHYSICS, CHEMISTRY, MATHEMATICS, 2020, 11 (5), P. 601–607

Synthesis and comparative photocatalytic activity of CuO layers on SiO_2 substrates

E. V. Polyakov, R. R. Tzukanov, I. V. Volkov, L. Yu. Buldakova, I. V. Baklanova, O. A. Lipina, V. P. Zhukov, Yu. V. Kuznetsova, A. P. Tutyunnik, M. A. Maximova

Institute of Solid State Chemistry UB RAS, 91, Pervomaiskaya str., Ekaterinburg, 620990, Russian Federation

polyakov@ihim.uran.ru

PACS 81.15.-z; 78.20.-e **DOI 10.17586/2220-8054-2020-11-5-601-607**

Using the thermodynamic and kinetic approaches, it was found that $Cu(NH_3)^{2+}_{4\,aq}$ complex predominating at 23°C spontaneously decomposes at elevated temperatures, forming CuO precipitate in a bulk solution and a layer ($CuO||SiO_2$) on the surface of silica glass. The rates of these heterogeneous processes are fairly well described by the 1st-order reaction of decay of the $Cu(NH_3)^{2+}_{4\,aq}$ complex. The formation of the CuO precipitate and layer is a two-step kinetic process. The rate of precipitate formation dominates above 65 °C while the rate of the layer formation prevails below this value. The $CuO||SiO_2$ material synthesized below 65° possesses an optical bandgap of (1.25±0.05) eV, which is smaller compared to the crystals of commercial CuO. The $CuO||SiO_2$ material displays a photocatalytic activity in the reaction of UV-decomposition of benzoquinone-hydroquinone. It was discovered that the photocatalytic activity depends on the thickness of the photocatalyst layer.

Keywords: Copper(II), oxide, layer, glass, surface, kinetics, photocatalyst.

Received: 18 September 2020

1. Introduction

A low efficiency of applied light utilization is considered to be the main drawback of powder photocatalysts. It can be improved by fixing micro- and nanoparticles of active material on substrates in the form of films and layers [1–3]. The properties of film photocatalysts depend on the accessibility of their surface for radiation, the morphology and size of surface particles and, consequently, on the conditions of synthesis. Among promising photocatalysts, CuO stands out as a p-type semiconductor with an optical gap width 1.21–1.51 eV that makes it active in the UV and visible spectral regions [4, 5]. CuO films allow utilization of up to 30% of incident light energy, which is much more compared to Cu_2O [6]. Synthesis of CuO layers in solutions [6–8] is a multistage process with the use of a solid-phase precursor $Cu(OH)_2$. The more simple and convenient method is the thermal decomposition of ammonia complexes of Cu(II) [9]. This unites the formation of primary CuO particles, their isolation and growth at the interface. The application of this method for the synthesis of photomaterials is restrained by the lack of information concerning synthesis conditions and the photocatalytic activity of produced CuO layers. The aim of present study was to invent a single-stage hydrochemical method for the production of CuO photocatalyst layers with optimal mass (thickness) on glass substrates by the thermal decomposition of ammonia complexes of Cu(II) in the conditions excluding the formation of Cu_2O.

2. Experimental work

Layer formation was studied by Dynamic Light Scattering (DLS) and Laser Doppler Electrophoresis measurements carried out on a Zetasizer Nano ZS particle analyzer (Malvern Panalytical Ltd.). The Raman spectral analysis of the samples was performed at room temperature using an inVia Reflex Renishaw spectrometer ($\lambda = 532$ nm, P=25 mW). The phase analysis of the products was fulfilled on a STADI-P X-ray powder automatic diffractometer (STOE) with CuKα1 radiation using the library of X-ray diffraction data PDF-2 (ICDD Release 2009). The morphology of the layers on substrate was studied using the scanning electron microscopy (SEM) and EDX elemental analysis on a JSM JEOL 6390LA facility. UV-visible absorption spectroscopy was performed using a Shimadzu UV-3101PC UV/Vis/Near-IR Spectrophotometer. The diffuse reflectance spectra of the layers were recorded in the interval of 220–800 nm by means of a Shimadzu UV-3600 UV-vis-NIR spectrophotometer using $BaSO_4$ crystals as a reference.

The thermodynamic study of the temperature evolution of CuO-$Cu(OH)_2$ phases in pH – Eh – temperature coordinates was carried out to choose the conditions of CuO formation in the bulk of electrolytic solution. The study was made for all known to date valence forms of copper. The HSC Chemistry v.8 program was used for the following equations (1–3):

$$Cu^{2+} + n NH_4OHCu(NH_3)^{2+}_n + n OH^-, \quad n = 3 - 5, \tag{1}$$

$$Cu(NH_3)^{2+}_n + (n+2)OH^- Cu(OH)_2(solution) + n NH_3 \times H_2O(aq), \tag{2}$$

$$\mathrm{Cu(NH_3)_n^{2+}} + (n+2)\mathrm{OH^-Cu(OH)_2} \,\|(interface) + n\mathrm{NH_3} \times \mathrm{H_2O}(aq). \quad (3)$$

The symbol "||(interface)" denotes the "solution – solid" interface. The pH-fields of predominance of 29 components including Cu^0, CuO, Cu_2O, $Cu(OH)_2$ phases, Cu(I,II,III) aqua-ions, their hydroxo-, mono- and dimeric ammonia complexes were determined as the function of a temperature. This allowed us to find the conditions for the spontaneous decomposition of $Cu(NH_3)_{4\ aq}^{2+}$ complexes which predominate in the reaction mixture at 23°. Thus, the complexes decompose at the temperature from 35 to 95° and pH from 11.0 to 12.0 with the generation of $Cu(OH)_2$ and CuO phases.

3. Results and discussion

3.1. Kinetics of CuO layers growth

According to the thermodynamic estimation by means of HSC Chemistry 8, $Cu(OH)_2$ to CuO transition in an Ar(g) atmosphere occurs at 150°. Under aerobic conditions, this decomposition takes place at 40–80° [8]. Hence, it is possible to control the solid phase precipitation rate in the bulk of solution and at the solution|| solid interface by choosing the synthesis conditions (temperature, solution chemistry and rate of solid phase formation) [9]. The search for synthesis conditions of CuO||SiO_2 layers on the inner surface of the quartz reactor (SiO_2) was carried out in 50 ml quartz vials filled with 25 ml 0.02–0.3 M copper(II) amine solution, C(Cu), with free ammonia concentration in the range of 0.4–4.0 M at thermostat temperature up to 95°. The synthesis took place according to reactions:

$$\mathrm{Cu(NH_3)_n^{2+}} + (n+2)\mathrm{OH^-} \overset{k(bulk)}{\longrightarrow} \mathrm{Cu(OH)_2/CuO}(bulk) + n\mathrm{NH_4OH}(aq), \quad (4)$$

$$\mathrm{Cu(NH_3)_n^{2+}} + (n+2)\mathrm{OH^-} \overset{k(interface)}{\longrightarrow} \mathrm{Cu(OH)_2/CuO||SiO_2}(interface) + n\mathrm{NH_4OH}(aq), \quad (5)$$

$$\frac{dC(Cu)}{dt} = -k(bulk, interface)C(Cu). \quad (6)$$

According to SEM, the produced CuO||SiO_2 layers consist of bundles of elongated particles having a form of nano-sheets. They first partially fill the surface of the glass and then grow normally to the surface. Fig. 1 shows that CuO particles anchored on the glass surface form an openwork layer in which particles alternate with uncovered glass "windows". The DLS data show that the colloidal CuO particles growing in the solution maintain a ξ-potential of -18.2 ± 26.3 mV throughout the synthesis, which indicates non-stable colloid solutions. In the initial 3–5 min period, the colloid particles have the hydrodynamic diameter of 90–100 nm and predominate in the solution. At the same time, the mean size of CuO particles anchored to the CuO||SiO_2 interphase keeps at the level of 280–290 nm. When the initial period ends, the size of CuO particles rises dramatically reaching the value of 1200 nm in the solution and 700–750 nm in the layer after 10–15 min synthesis, Fig. 2. The kinetic coefficients of direct reactions (4–6) were determined experimentally. For this purpose, the variation with time of the copper content in solution (I), on the inner surface of vial (II) and in the precipitate after removal of copper by filtration (III) was analyzed using the mass spectrometry method (Elan 9000), Fig. 3. The characteristics of the compositions were fairly well confirmed by means of spectroscopy and X-ray diffraction analysis (XDA). The Raman spectrum of composition (II) contains vibrational modes of CuO: 282 cm^{-1} (A_g), 332 cm^{-1} and 616 cm^{-1} (B_g) [4]. For composition (III), the vibrational modes of CuO are shifted relative to (II): 303 cm^{-1} (A_g), 350 cm^{-1} and 636 cm^{-1} (B_g) [11]. The XDA reflections of compositions (II) and (III) are identical to those of CuO phase: space group C12/c1, lattice parameters a = 4.6804, b = 3.4337, c = 5.1164, α = 90.0000, β = 99.1329, γ = 90.0000. The X-ray density of CuO in the layer is 6.490 g/cm^3 and the mean crystallite size, calculated using the Scherrer equation, is 27.1–27.9 nm.

The least squares method was applied to estimate the coefficients of formation rate (6) in the bulk, *k(bulk)*, and at the solution-glass interface, *k(interface)*, at 23–85°. The data obtained allowed us to identify the temperature region (below 65°), in which the reaction (4) of the layer growth predominates (Fig. 3, marked by arrow). Thus, the series of CuO||SiO_2 materials with different CuO layer thickness were synthesized on the surface of glass and used in further photocatalytic measurements. The synthesis conditions to achieve optimal degree (60–80%) of copper(II) ions transformed into oxide were chosen as follows: 35–65° temperature interval, 15–60 min synthesis time. The photocatalytic effectiveness of studied materials is demonstrated by the UV-visible diffuse reflectance spectroscopy data. The results show that the optical bandgap E(eV) calculated by means of the Kubelka-Munk equation for a direct transition in CuO crystals (see [10–12]) is equal to 1.25 ± 0.05 eV for the CuO||SiO_2 materials, whereas for commercial CuO it is around 1.50 ± 0.05 eV [13]. The absence of the Cu_2O phase in the layers was additionally confirmed by the voltammetry method [14] using the discussed copper(II) oxide layer deposited on the surface of Ni-foil electrode.

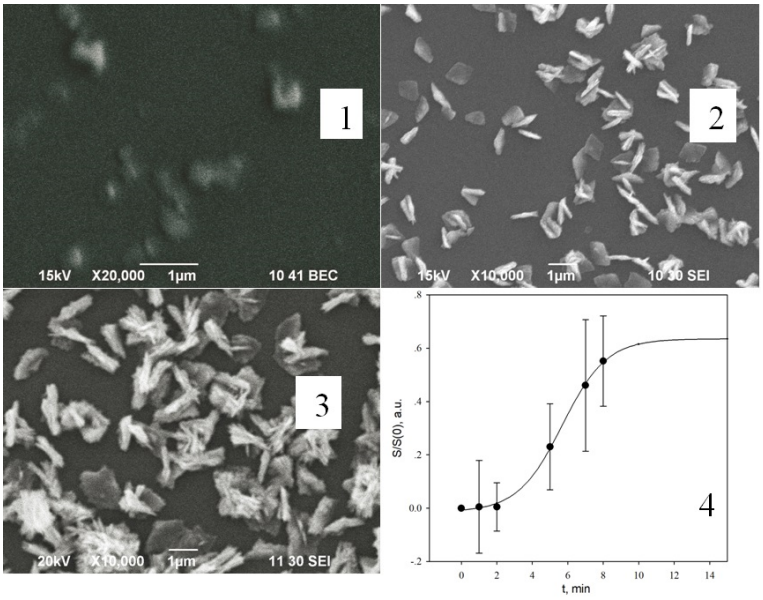

FIG. 1. Size and morphology of CuO particles forming a layer on the surface of quartz vial (CuO||SiO_2) at different times of synthesis: 1 – 0.5 min; 2 – 3 min; 3 – 5 min. Panel 4: variation of relative coverage S/S(0) of SiO_2 surface with CuO particles as a function of reaction time t. S – surface of SEM image of quartz vial covered with CuO particles (μm^2), S(0) – total surface of the same image (μm^2). Temperature of synthesis is 85 °C

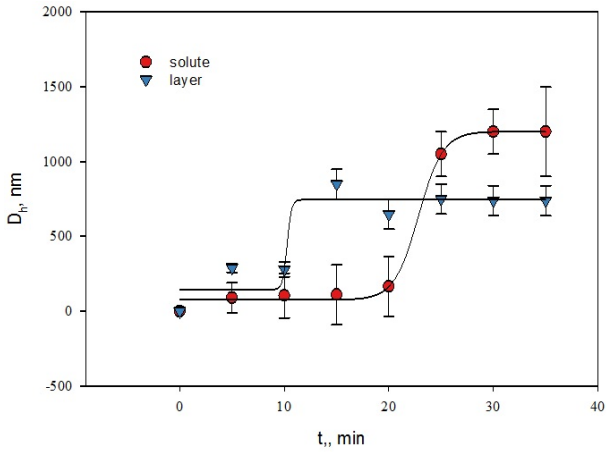

FIG. 2. Variation of CuO particles diameter (D_h) in bulk solution (solute) and in the interface solution||layer (layer) during $Cu(NH_3)_4^{2+}$ ion particles deposition acquired with the help of dynamic light scattering and laser Doppler electrophoresis measurements. 85 °C

3.2. Photocatalytic activity of CuO layers on the silica glass

The photocatalytic activity of synthesized CuO layers of different thickness on the inner surface of quartz reactor walls was analyzed under the UV irradiation in the reaction of the decomposition of the electrochemically reversible pair of benzoquinone–hydroquinone, BQ-HQ. For this purpose, 25 ml BQ-HQ solution with initial concentration C_s° = 0.1 mM at pH = 6.8, 22° was poured into quartz vials lined with CuO. A UV lamp was mounted above the reactor so that the UV-irradiation propagated from top to the bottom of reactor both through the "solution-air" interface (UV-light flow F1) and through the "CuO||SiO_2 – solution" interface (UV-light flow F2) [15]. The scheme of the interaction of UV-light flows F1, F2 with thin (A) and thick (B) layers of CuO is depicted in Fig. 4a,b. Before each experiment, the BQ-HQ solution was contacting with CuO layer for a time needed to reach equilibrium absorption of BQ-HQ on the surface of the photocatalyst. The experiments have shown that adsorption equilibrium state was reached in 25–30 minutes. After that each of the quartz reactors was irradiated with UV light of the wavelength λ(max) = 253 nm

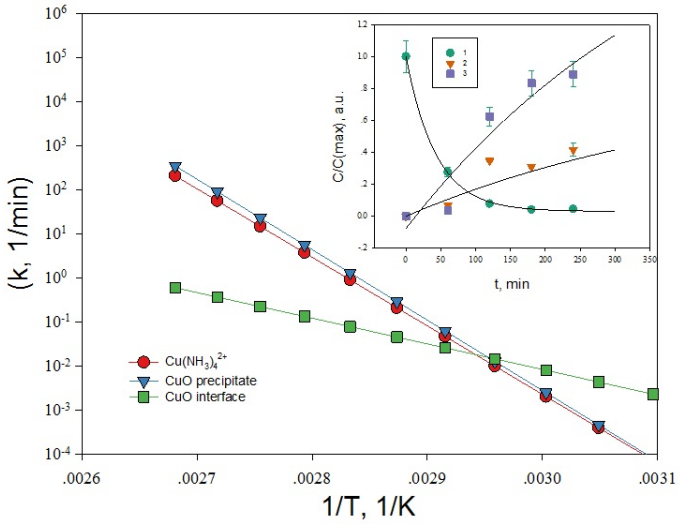

FIG. 3. Temperature dependence of kinetic coefficients of eq. 6 which describe solid phase formation according to 1st order reactions (4–5), calculated from experimental data (inset). T is the temperature of thermo-decay. On the inset the examples are shown of the kinetics of $Cu(NH_3)_4^{2+}$ thermo-decay in NH_4OH solution as a functions of contacting time. Initial Cu(II) concentration in the solution $C(\max) = 0.02$ M, pH = 11.3, 70 °C, volume of solution = 25 ml. Concentration in the phases (M units) is calculated as a ratio of Cu mass in the phase to the volume of solution; 1 – in solution, 2 – in precipitate, 3 – in vial coating. Solid lines represent the least square curve fit of the data in accordance with simple 1st-order decay/formation model. An arrow points out the temperature 65 °

(4.9 eV) using the technique described elsewhere [15]. The substrate concentration variation (C_s) with irradiation time (t) in the series of experiments with the CuO layers of a different thickness is found (see Fig. 4c) to obey the 1st-order decay reaction equation (6):

$$\begin{array}{l}(BQ - HQ) + h\nu \xrightarrow{k} products, \\ dC_s/dt = -k_s C_s\end{array} . \qquad (7)$$

In eq. (7), k_s is the rate constant, which depends on the quantum yield of the photocatalytic reaction. The geometric thickness of the layers (L, nm) was determined by EDX analysis of CuO||SiO_2 composites on a JSM JEOL 6390LA facility. The experimental correlation between the relative rate constant k_s/k_s(max) and L, where k_s(max) is the maximal value of constant (k_s) in the series of layered photocatalysts, is shown in Fig. 5. It is seen that k_s/k_s(max) keeps the maximal value in the series of rather thin CuO layers with $L < 1000$ nm. This conforms to the results of quantum-chemical simulation of UV radiation absorption by monocrystalline CuO, which we performed with the use of the VASP program [16], Fig. 6. The calculated variation in the relative light transmission $I(L_c)/I(0)$ of UV radiation as a function of the light path length in the catalyst crystal (L_c) strongly depends on the radiation energy (E). The calculated data show that 99% of UV-radiation with $E > 3.5$ eV are absorbed within the thin CuO crystal layer with $L_c \sim$ 80–100 nm. Since the thickness of sheet-like bundles of CuO particles is $\sim$ 200–250 nm, Fig. 1, one can conclude that all photon energy of UV-light are absorbed by CuO sheet-like particles of the CuO||SiO_2 photocatalyst independently of its thickness. Nevertheless, when the experimental layer thickness L increases, the k_s/k_s(max) value decreases to a constant level, which is characteristic of micro-sized particles of CuO. To understand this phenomenon, the UV-light flow geometry and the morphology of CuO layers growing on the glass support were taken into consideration. In accordance with experimental conditions, there were two components of general UV irradiation flow, Fig. 4a,b. Fraction F1 of the flow kept a constant intensity since it passed through air/solution interface which was free of the colloid particles and CuO layer. Fraction F2 of the flow passed through the side walls of the quartz vial. As a result, its intensity depended on the thickness and transparency of the growing layer. Fig. 1 shows that the layers of CuO photocatalyst have openwork morphology. This implies that the rather small thickness of layer leads to the formation of "windows" in the silica glass. These regions of the substrate are not covered with CuO particles and freely transmit UV irradiation which scatters on and interact with the CuO nano-sheets surface. When the thickness of photocatalyst layer reaches a rather large value L(max), the surface of "windows" diminishes and the

UV-light flow F2 attains its minimal (or zero) value. In the framework of this interpretation, the value of L(max) is about 10^4 nm. The frontier divided these two regions is shown in Fig. 5.

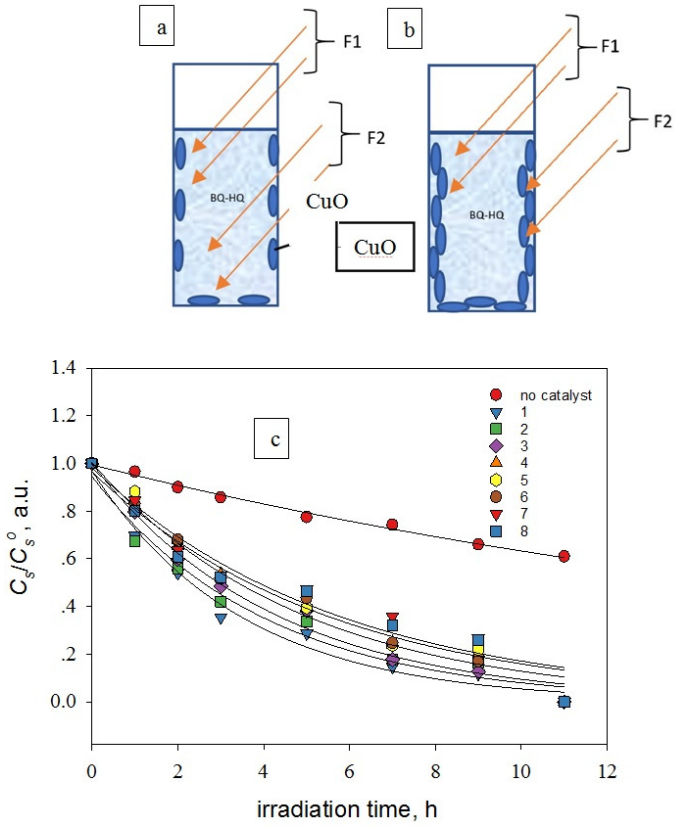

FIG. 4. Photocatalytic decomposition of 0.1 mM solution of BQ-HQ on the layers of catalyst CuO deposited on the vials inner surface as a function of irradiation time. (a, b) – the schemes of UV-irradiation of CuO on the surface of vials in the case of thin (a) and thick (b) layers. (c) – Decomposition of substrate under UV light as a function of irradiation time. Numbers near the pointers are for the catalyst layers thickness (nm): 1 – 1500, 2 – 1650, 3 – 6020, 4 – 9400, 5 – 12700, 6 – 14600, 7 – 17900, 8 – 24800. Volume of substrate solution is 25 ml, measurements at 22 °C, UV light energy – 4.90 eV. Solid lines are the best fit approximation of the substrate decomposition in accordance with eq. (6). The surface area of the glass support in each sample was constant and equal to 4.2 cm^2

4. Conclusion

Thus, using thermodynamic and kinetic approaches, it was found that the $Cu(NH_3)^{2+}_{4\ aq}$ complex predominating at 23° spontaneously decomposes at elevated temperature with the deposition of CuO phase in the form of the precipitate in a bulk solution and layer on the surface of silica glass (CuO||SiO_2). The rates of these heterogeneous processes are described by the 1st-order reaction of the decay of the $Cu(NH_3)^{2+}_{4\ aq}$ complex. It was found that the formation of CuO precipitate and a layer is a two-step kinetic process. The rate of precipitate formation predominates above 65° while the rate of CuO layer formation prevails below 65°. CuO||SiO_2 synthetized below 65° possesses an optical bandgap of (1.25±0.05) eV which is smaller in comparison with commercially-available CuO crystals. The samples of CuO||SiO_2 material display the photocatalytic activity in the reaction of UV-decomposition of benzoquinone-hydroquinone. Wherein, the activity depends on the thickness and morphology of the photocatalyst layer.

Acknowledgements

This study has been performed in the framework of the State research program. The calculations were carried out on the URAN cluster at the Institute of Mathematics and Mechanics of the Ural Branch of the Russian Academy of Sciences.

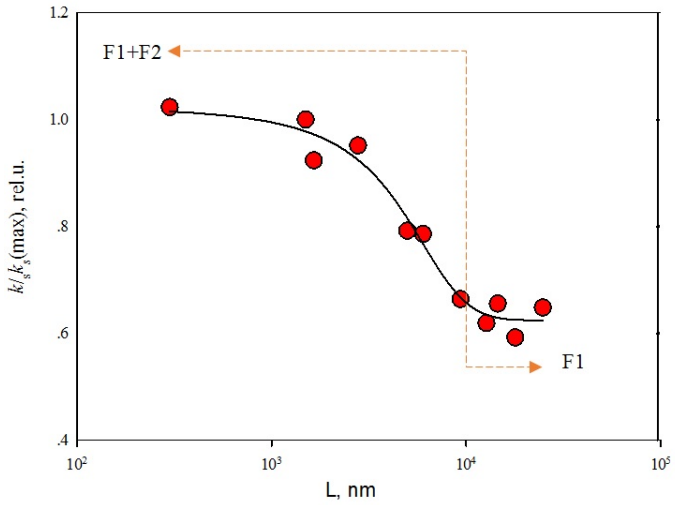

FIG. 5. Correlation between experimentally estimated rate constant of photo-degradation of substrate (k_s) according to eq. (6) and thickness of photocatalyst CuO layer (L) in the series of composites CuO||SiO_2. $k_s(\max) = 8.20 \cdot 10^{-5}$ 1/c, 22 °C. Vertical dotted line separate areas of thickness L within which the whole incident UV light flow is active ($L < 104$ nm) or only its F1 component ($L > 104$ nm) can penetrate through the CuO layer (see Fig. 4)

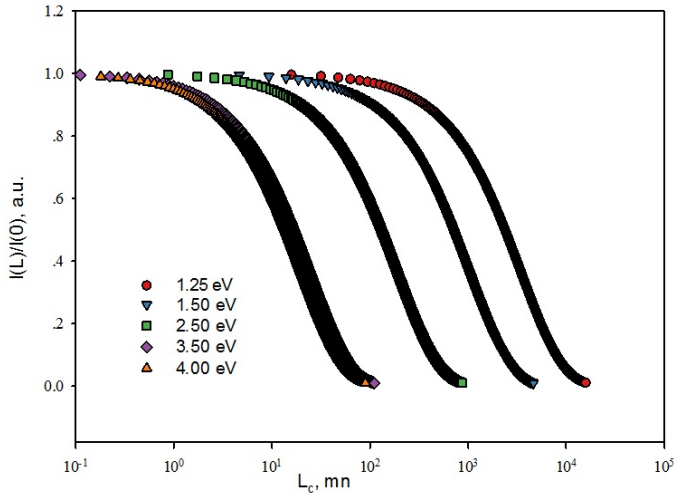

FIG. 6. The relative intensity $I(L)/I(0)$ of light transmitted to the depth L_c in CuO with respect to the intensity at the surface $I(0)$, as determined by means of the VASP computer code [16]

References

[1] Ochiai T., Fujishima A., J. Photoelectrochemical properties of TiO_2 photocatalyst and its applications for environmental purification. *Journal of Photochemistry and Photobiology C: Photochemistry Reviews*, 2012, **13**, P. 247–262.

[2] Varshney G., Kanel S.R., Kempisty D.M., Varshney V., Agrawale A., Sahle-Demessie E., Varmac R.S., Nadagouda M.N. Nanoscale TiO_2 films and their application in remediation of organic pollutants. *Coordination Chemistry Reviews*, 2016, **306**, P. 43–64.

[3] Lai Ch.W., Lee K.M., Juan J.Ch. Chapter 7. Polymeric Nanocomposites for Visible-Light-Induced Photocatalysis. M.M. Khan et al. (eds.). *Nanocomposites for Visible Light-induced Photocatalysis. Springer Series on Polymer and Composite Materials*. Springer International Publishing AG, 2017.

[4] Cheng G. Synthesis and characterisation of CuO nanorods via a hydrothermal method. *Micro and Nano Letters*, 2011, **6**, P. 774.

[5] Tuerdi A., Abdukayum A., Chen P. Systhesis of composite photocatalyst based on the ordered mesoporous carbon-CuO nanocomplex. *Materials Letters*, 2017, **209**, P. 235–239.

[6] Chuantian Z., Ding, Liming L. Solution-Processed Cu_2O and CuO as Hole Transport Materials for Efficient Perovskite Solar Cells. *Small*, 2015, **11**, P. 5528–5532.

[7] Kakhki R.M., Ahsani F., Mir N. Enhanced photocatalytic activity of CuO-SiO_2 nanocomposite based on a new Cu nanocomplex. *Journal of Materials Science: Materials in Electronics*, 2016, **27**, P. 11509–11517.

[8] Lim Y.-F., Choi J.J., Hanrath T. Synthesis of Colloidal CuO Nanocrystals for Light-Harvesting Applications. *Journal of Nanomaterials*, 2012, **2012**, P. 1–6.
[9] Mokrushin S.G., Kitaev G.A. Experimental investigation into laminar systems. *Kolloidnyi Zhurnal*, 1957, **19**, P. 93.
[10] Brodie-Linder N., Audonnet F., Deschamps J., Alba-Simionesco C., Besse R., LeCaer S., Impéror-Clerc M. The key to control Cu II loading in silica based mesoporous materials. *Microporous and Mesoporous Materials*, 2010, **132**, P. 518–525.
[11] Irwin J.C., Chzhanovski J., Wei T., Lockwood D.J., Wold A. Raman scattering from single crystals of cupric oxide. Physica C, 1990, 166, P. 456–464.
[12] Kubelka P., Munk F. An article on optics of paint layers. *Zeitschrift für technische Physik*, 1931, **12**, P. 593–609.
[13] West A. R. *Solid State Chemistry and Its Applications*. New Jersey, Wiley, 1987, 742 p.
[14] Polyakov E.V., Denisova T.A., Maksimova L.G., Zhuravlev N.A., Buldakova L.Yu. Hydrogen and salt forms of tin ferrocyanide as precursors of mixed ferrocyanides. *Russian Journal of Inorganic Chemistry*, 2000, **45**, P. 276–282.
[15] Polyakov E.V., Krasilnikov V.N., Gyrdasova O.I., Buldakova L.Yu., Yanchenko M.Yu. Synthesis and photocatalytic activity of quasi-one-dimensional (1-D) solid solutions $Ti_{1-X}MXO_{2-2X/2}$ (M(III)= Fe(III), Ce(III), Er(III), Tb(III), Eu(III), Nd(III) and Sm(III), $0 \leq X \leq 0.1$). *Nanosystems: Physics, Chemistry, Mathematics*, 2014, **5**, P. 553–563.
[16] G. Kresse, J. Furthmuller. Vasp the guide. Vasp the guide. Homepage. 2011. (http://cms.mpi.univie.ac.at/vasp/guide/vasp.html).